Case Studies in Thermal Engineering 21 (2020) 100655

Contents lists available at ScienceDirect

Case Studies in Thermal Engineering

journal homepage: http://www.elsevier.com/locate/csite

Performance of beeswax phase change material (PCM) and heat pipe as passive battery cooling system for electric vehicles

Nandy Putra [a,*], Adjie Fahrizal Sandi [a], Bambang Ariantara [a,b], Nasruddin Abdullah [a,c], Teuku Meurah Indra Mahlia [d]

[a] Applied Heat Transfer Research Group, Department of Mechanical Engineering, Faculty of Engineering, Universitas Indonesia, Kampus UI Depok, Jawa Barat, 16424, Indonesia
[b] Mechanical Engineering Department, Faculty of Engineering, Universitas Pasundan, Jl. Setiabudi 193 Bandung, 40153, Indonesia
[c] Department of Mechanical Engineering, Universitas Samudra, Aceh, 24411, Indonesia
[d] School of Information, Systems and Modelling, Faculty of Engineering and Information Technology, University of Technology Sydney, NSW, 2007, Australia

ARTICLE INFO

Keywords:
Phase change material
Heat pipe
Battery
Passive cooling system

ABSTRACT

Increasing greenhouse gas (GHG) emissions in the atmosphere and the scarcity of fossil fuel sources have encouraged car manufacturers to develop more environmentally friendly electric vehicles (EVs). The technology advancements of EVs—those with battery systems in particular—have increased their travel distances. Therefore, increasing and maintaining the battery capacity is a key concern in the development of sustainable EVs. In this study, passive cooling systems were constructed with a heat pipe and phase change material (PCM), and their performances were investigated with battery simulators. The aim was to determine the effectiveness of the cooling system and to identify the optimal PCM (beeswax or Rubitherm RT 44 HC) for a temperature range of 25–55 °C. The use of a heat pipe could decrease the battery temperature by 26.62 °C under a 60 W heat load compared to the case without passive cooling system. Furthermore, the addition of RT 44 to a heat pipe resulted in a maximal temperature decrease of 33.42 °C. Thus, an RT 44 HC is more effective than beeswax because its melting temperature lies within the recommended range of the battery working temperature, and its latent heat allows the absorption of more heat compared to beeswax.

1. Introduction

Owing to the extensive use of fossil fuels, greenhouse gas (GHG) emissions—carbon dioxide (CO_2) emissions in particular—have increased tremendously in the atmosphere and drove scientists to find solutions [1]. Many solutions have been presented for this problem, such as using renewable energy sources [2,3], biofuel [4] and energy-efficient policies [5–7]. However, some renewable energies (e.g. solar and wind energy) are only available during specific times. One of the solutions for this problem is to store energy in, e.g. batteries. However, this solution is limited in terms of storage capacity and material availability. Another popular solution employs phase change materials (PCMs). One of the study attempts to characterized and analyse the thermal properties of nanoencapsulation

* Corresponding author. Department of Mechanical Engineering, Faculty of Engineering, Universitas Indonesia, 16424, Depok, West Java, Indonesia.
E-mail address: nandyputra@eng.ui.ac.id (N. Putra).

https://doi.org/10.1016/j.csite.2020.100655
Received 9 February 2020; Received in revised form 10 May 2020; Accepted 12 May 2020
Available online 16 May 2020

Nomenclatures

Q :	total absorbed heat (W)
m :	mass (kg)
C_p :	specific heat
Q_{in}	heat transferred by the heat pipe (W)
R_{st}	thermal resistance (K/W)
T_e	$T_{evaporator\ average}$ (^oC)
T_c	$T_{condensor\ average}$ (^oC)
T_i :	initial temperature (^oC)
T_m :	melting temperature (^oC)
T_f :	final temperature (^oC)
Δh_m :	latent heat (kJ)

phase change materials via sol-gel method [8]. Then following by the preparation and characterization of palmitic acid/graphene nanoplatelets composite with a remarkable thermal conductivity as a novel shape-stabilized PCM [9]. The research quite encouraging but did not give an optimized result and therefore Amin et al. [10] attempt to analyse a new material from beeswax/graphene thermal as PCM. This research then following by using beeswax/multi-walled carbon nanotubes and attempted to used novel thermoelectric module based devices for thermal stability measurement of PCM [11,12].

One of the reasons for global warming is the increasing number of vehicle owners each year, which has consequences for emissions and fuel availability [13]. Therefore, the interest in electric vehicles (EVs), including hybrid EVs (HEVs) and plug-in HEVs (PHEVs), has significantly increased as environmental regulations on GHG emissions have been tightened. The development of EVs represents one approach to reduce CO_2 emissions in the transportation sector. In addition to reducing emissions, EVs reduce the consumption of fossil fuels, which are non-renewable energy sources.

In general, the introduction of EVs for mass transportation has not affected owners of conventional vehicles. One of the reasons is the limited ability of EV batteries. These batteries have high-performance characteristics, including high specific energy, longer life cycle, and short charging time. Research on these batteries must be continued before EVs can substitute conventional cars. Currently, lithium-ion batteries are the most common choice for energy storage. They offer specific energies of 110–180 Wh/kg, lifetimes of more than 1000 cycles, and charging times of 2–3 h [14]. To maintain the battery properties, which is crucial for sustainable EVs, the battery temperature should remain between 25 °C and 55 °C [15].

To maintain the battery temperature in the optimal operating range, EV manufacturers are developing cooling systems for batteries. Some methods have been proposed to manage the heat released by a battery during its working process, e. g. air-cooled and liquid-cooled battery systems and PCMs [16–18]. Fan et al. [19] successfully used air-cooled for hybrid electric vehicle lithium-ion battery while Mohammadian et al. [20] discussed hybrid electric vehicles thermal management of an air-cooled Li-ion battery. The efficiency of air-cooled battery thermal management has been improved through the improvement of the pattern of flow [18]. Where liquid-cooled battery has been discussed by Rao et al. [21]about implementing liquid cooling based thermal management for Lithium-ion battery, where Li et al. [22], successfully used water for Lithium-ion battery cooling system and Xu et al. [23], applied double-inlet and double-outlet channels for cooling electric vehicle battery using a liquid cooling system. The PCMs have also been used by many researchers such as, by Chen et al. [18] conducted the experiment on PCM-heat pipe to cool power battery packs of a car. Meanwhile, Bai et al. [17] combine water and PCM for cooling Lithium-ion batteries. However, the most complete discussion on the subject presented by Akeiber et al. [16] who conducted a review on every aspect of using PCM for passive cooling.

Active cooling systems such as air-cooled circulating water and cooling towers are still used to cool EV batteries. The air-cooled battery cooling system is influenced by an extended surface and turbulence flow pattern, and forced convection is used to increase the convection heat transfer coefficient. However, the heat can usually not be dissipated timely from the battery module to the ambient air, which has a poor heat transfer coefficient. Thus, air-cooled systems cannot meet the temperature requirements of these batteries.

Liquid cooling is another method that effectively reduces the surface temperature of a battery module. However, the method requires a more complicated system and equipment (e.g. a pump and pipe system) and is, therefore, more expensive. Moreover, if the liquid leaks from the pipe, the battery becomes easily short-circuited.

Alternatively, passive cooling systems such as heat pipes can be used to control the battery temperature which has been discussed by Putra et al. [24]. In their research, batteries of the electric vehicle have been cooled using heat pipes as heat exchangers. The flat plate loop heat pipe (FPLHP) in the thermal management for lithium-ion batteries. The working fluids used in this study are distilled water, alcohol, and acetone with 60% filling ratio. The study found the best performance of all working fluid is acetone which yields 0.22 W/°C of thermal resistance with the evaporator temperature at heat and flux load of 50 °C and 1.61 W/cm^2, respectively. A heat pipe is a conductor consisting of a metal tube, capillary wick, and working fluid inside the pipe under vacuum conditions. A straight heat pipe has a high equivalent thermal conductivity (approximately 3.8×10^4 W/m.K). Thus, it can transfer heat much faster than copper bars of equal dimensions [25].

Phase change materials (PCMs) are widely used to control temperatures based on latent heat. They have excellent thermal energy storage properties because they use sensible and latent heat. The level of latent heat depends on the type of PCM [16]. For example, Amin et al. [10] reported a latent heat of 141.49 kJ/kg and a melting point of 62.28 °C for beeswax. However, the properties of paraffin

PCMs depend on the number of carbon chains. Rao et al. [26] used paraffin as PCM with water mini channels. The best cooling performance was obtained with eight channels with a mass water flowrate of 8×10^{-4} kg/s and a PCM with a phase change temperature of 308.15 K and thermal conductivity of 0.6 W/m.K. Furthermore, Wang et al. [27] immersed a battery in paraffin and added a fin to the battery surface to control the battery temperature, which decreased with increasing fin number. One drawback of PCMs is their low thermal conductivity. To overcome this problem, Wu et al. [28] added a porous copper sheet to paraffin, which enhanced the thermal conductivity from 0.26 to 7.65 W/m.K and decreased the surface temperature of the battery by 3.9 °C.

Several researchers have evaluated heat pipe-assisted PCMs as passive cooling systems for batteries. To control the temperature of a cylindrical battery, Zao et al. used six cylindrical heat pipes and fins and immersed the battery in paraffin. They achieved a temperature reduction of 5 °C and maintained the battery temperature at values below 50 °C. Huang et al. [29] developed a flat heat pipe-assisted PCM and investigated thermal management systems with serial-PCM-based batteries for cylindrical lithium battery modules. They included pure PCMs, heat pipe-coupled and air-assisted PCMs (PCM/HP-Air), and heat pipe-coupled and liquid-assisted PCMs (PCM/HP-Liquid). Their results showed that the heat pipe played an important role in transporting the heat promptly in the PCM-based battery module. Moreover, the heat pipe-assisted PCM-based battery thermal management system exhibited excellent thermal performance. Moreover, Wu et al. [30] investigated the thermal performance of heat pipe-assisted PCM plate-based battery thermal management systems. They employed L-shaped heat pipes and paraffin/expanded graphite as PCM. During their experiments, the heat generated within the batteries was first absorbed by the PCM and then conducted through the evaporator section to the condenser section of the heat pipe. According to their results, the proposed system achieved maximal temperatures below 50 °C. Recently, Zhang

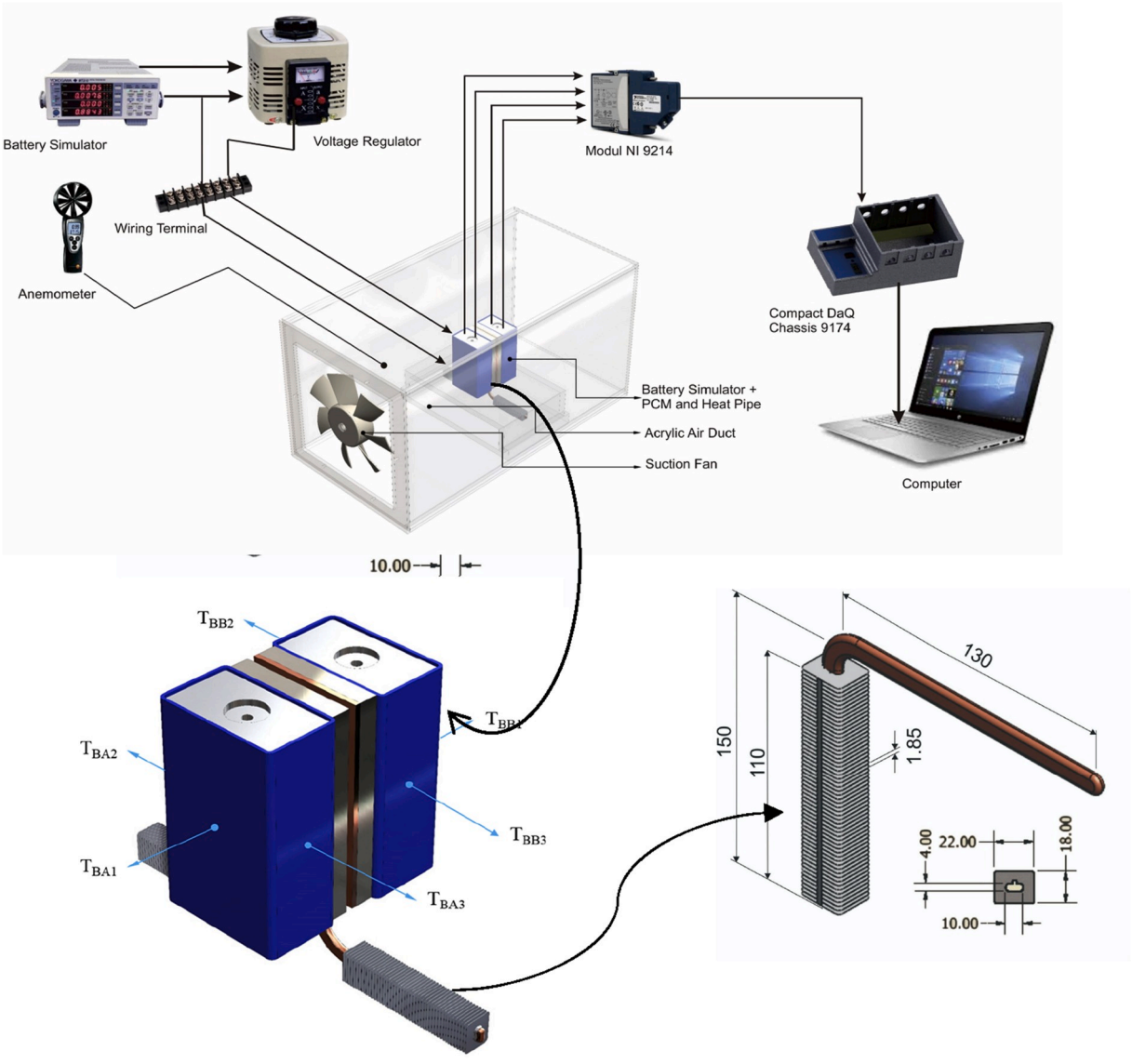

Fig. 1. Experimental setup and Positions of thermocouples.

et al., 2020 [31] have conducted research on battery thermal management system (BTMS) that combines heat pipes, copper foam and PCM in order to balance the temperature in a LiFePO4 battery pack. In that research, the generated heat from battery is transferred in serial configuration, first transmitted through heat pipes, and then is absorbed by the phase change material then dissipated to the environment. Their results showed that the proposed system offers a more suitable temperature under 45 °C, which is considered as the highest temperature of the optimum operating temperature range.

In this paper, a passive cooling system based on finned L-shaped heat pipes and PCM is proposed for a battery module. PCM and heat pipes are arranged in parallel, where the heat from the battery on one side is absorbed by the heat pipe and on the other side is absorbed by PCM and together released into the surrounding air. The low thermal conductivity of PCM will not dramatically reduce the overall thermal resistance. A parallel configuration will produce a lower overall thermal resistance than a serial configuration. The thermal performances of battery modules of three different thermal management systems were compared: without heat pipe and PCM, with heat pipe, and heat pipe-coupled with PCM. Furthermore, beeswax and the Rubitherm RT 44 HC were selected as PCMs for the thermal management of a power battery.

The objectives of our study were: (1) determining the effectiveness of a heat pipe as a passive battery cooling system; (2) evaluating the ability of both heat pipe and PCM to reduce the battery temperature; (3) determining the optimal PCM for passive battery cooling. The equipment is an integrated PCM and finned L-shaped heat pipe for a passive battery cooling system. To the best of our knowledge, few studies have been performed on the development of integrated PCMs and finned L-shaped heat pipes in cooling applications.

2. Experiments

2.1. Experimental components

An integrated PCM and finned L-shaped heat pipe will be applied for EVs. Because of the limited space in EVs, the battery cooling system must be compact and well-designed. The test cell of the integrated PCM and finned L-shaped heat pipe consist of three main components: (1) two battery simulators with a heater and stainless-steel conductor, (2) PCM container, and (3) two finned L-shaped heat pipes. The battery simulators are made from stainless steel and have dimensions of 137 × 82.5 × 46 (mm^3). A heater was placed inside each battery simulator to simulate the heat generation in a real lithium-ion battery. Thus, the heat load of the battery simulator could be controlled with a voltage regulator. The stainless-steel plate was inserted between the heat pipe holder and battery simulator. The heat transferred to the heat pipe can be obtained by determining the temperature difference across the plates with the Fourier heat conduction equation.

In the experiment, two battery simulators and conductors with heaters were placed inside an air duct. The heat generated by the heater was transferred to the battery simulator and increased its temperature. Furthermore, the heat pipes were placed in a heat pipe holder between the battery simulators. The thermal conductivity of the stainless-steel conductors was assumed to be 16.2 W/m.K [32]. Stainless steel was chosen owing to its sufficiently low thermal conductivity. Thus, the temperature difference between the surfaces could be measured.

In this study, the battery simulator temperature was controlled by the heat pipe and PCM. Heat pipes have a very high equivalent thermal conductivity because the heat transfer involves phase changes in the working fluid. The heat pipe has two components—an evaporator and a condenser—and the fluid flow is a two-phase flow. The working fluid is in the liquid phase in the evaporator and in the vapor phase in the condenser. The PCM uses both sensible and latent heats for the thermal storage, which results in efficient thermal energy storage. Thus, the primary strategy to control the battery temperature is to quickly transport the battery heat to the environment through the heat pipe and to simultaneously adsorb the heat with the PCM.

The employed heat pipes were finned L-shaped heat pipes with water as working fluid (filling ratio of 50%). Their geometries and dimensions can be seen in Fig. 1. Fins were added to the condenser section to increase the total contact area, thereby increasing the convection rate between the heat pipe and air moved by the fan. The evaporator sides of two heat pipes were placed on a copper heat pipe holder to obtain a good contact surface between the battery simulator and heater. The performance of the heat pipe depends on its properties, e.g. its thermal resistance. A heat pipe with a low thermal resistance performs best because it can transfer heat quickly. The thermal resistance (*Res*) can be calculated from the temperature difference between the evaporator and condenser and the heat transferred by the heat pipe [33]:

$$Res = \frac{T_{\text{evaporator average}} - T_{\text{condenser average}}}{Q_{in}}. \quad (1)$$

Table 1
Thermal properties of Beeswax and RT 44 HC

Property	RT 44 HC	Beeswax
Melting temperature (°C)	44 [18]	62.28 [9]
Latent heat (kJ/kg)	250 [18]	141.49 (liquid) [9] 145. 62 (solid) [9]
Density (kg/m^3)	700 (liquid) [18] 800 (solid) [18]	789.47 (liquid) [9] 819.75 (solid) [9]
Thermal conductivity (W/m K)	0.23 [18]	0.25 [9]

Two PCM types with different melting temperatures were used in this study: (1) an RT 44 HH, the melting temperature of which is within the desired working temperature of the battery [34] (2) beeswax [10], the melting temperature of which exceeds the desired working temperature of the battery (Table 1). A total PCM mass of 0.4 kg was added to the battery. To ensure that the PCM was evenly spread, the PCM was used in its liquid phase (i.e. heated to its melting point), to let it flow over the battery box.

The heat absorbed by the PCM increased the PCM temperature and phase change. The total energy can be calculated with:

$$Q = \int_{T_i}^{T_m} m\, C_p\, dT + m\, \Delta h_m + \int_{T_m}^{T_f} m\, C_p\, dT. \tag{2}$$

2.2. Experimental setup

The surface temperature of the battery was measured with 0.3 mm in diameter K-type thermocouples, which were attached to the surface centre of each battery simulator, PCM, and heat pipe surface to record the temperature with a PC-based data acquisition unit (NI System). Their positions are shown in Fig. 1. All thermocouples were calibrated in the temperature range 0–100 oCwith standard thermometer, before the experiment and they have accuracy of ±0.05 °C. The thermal energy of the battery simulator was controlled with a voltage regulator (Yokogawa WT310; the accuracy of ±0.1%). Moreover, a fan was used to blow the air through the finned array of the L-shaped heat pipe for forced air convection. The velocity of the flowing air through the condenser section of the HP was measured with a hot-wire anemometer. The uncertainties can be calculated based on the uncertainties of the primary quantities. The uncertainty present in the estimation of thermal resistance of HP was calculated as

$$\frac{\Delta R_{Th}}{R_{Th}} = \sqrt{\left(\frac{\Delta(Te - Tc)}{(Te - Tc)}\right)^2 + \left(\frac{\Delta Q}{Q}\right)^2} \tag{3}$$

Thus, the resulting uncertainty of the thermal resistance of the HP was estimated to be within ±2%. The experimental setup is depicted in Fig. 1.

2.3. Experimental procedure

These experiments were conducted to evaluate the performance of the PCM and heat pipes regarding the reduction of the battery surface temperature. First, the battery simulator was run for 5500 s without a heat pipe or PCM to determine the maximal battery simulator temperature. Subsequently, the heat pipes were installed on the battery simulators, and the battery simulator temperature was measured to determine the effect of the heat pipe on the battery temperature. Next, the battery and heat pipes were covered with PCM as a passive cooling system. Moreover, the PCM (Beeswax or RT 44 HC) was poured into the battery box. The PCM covered the entire battery surface. Thus, the thermal energy on the entire battery surface could be absorbed. In the experiments, the battery simulator was heated with heat loads of 40, 50, and 60 W for 5500 s.

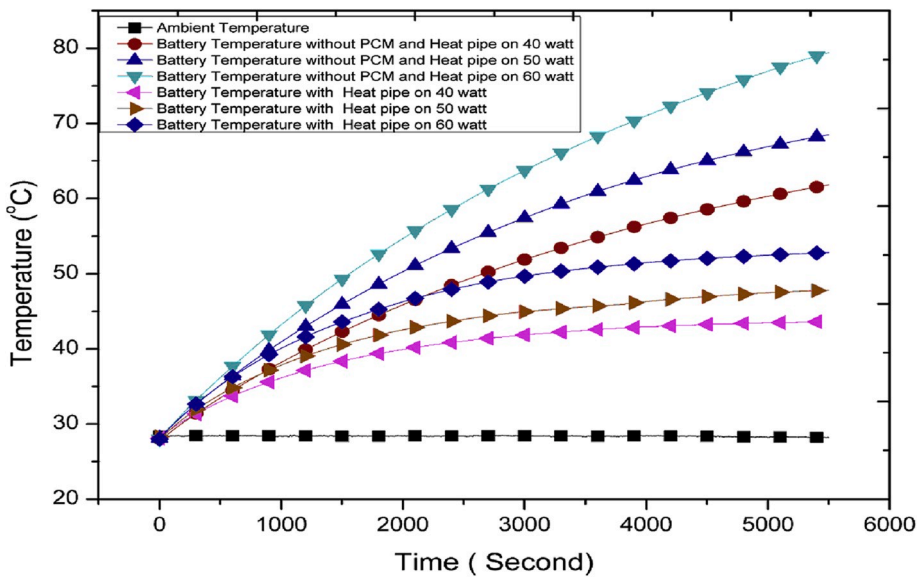

Fig. 2. Battery simulator surface temperature with and without heat pipes.

3. Results and discussion

3.1. Heat pipe performance

The heat generated by the heater caused the battery surface temperature to increase. Owing to the high thermal conductivity of the heat pipe, the battery heat was quickly absorbed and transferred to the air. Fig. 2 shows the battery surface temperatures with and

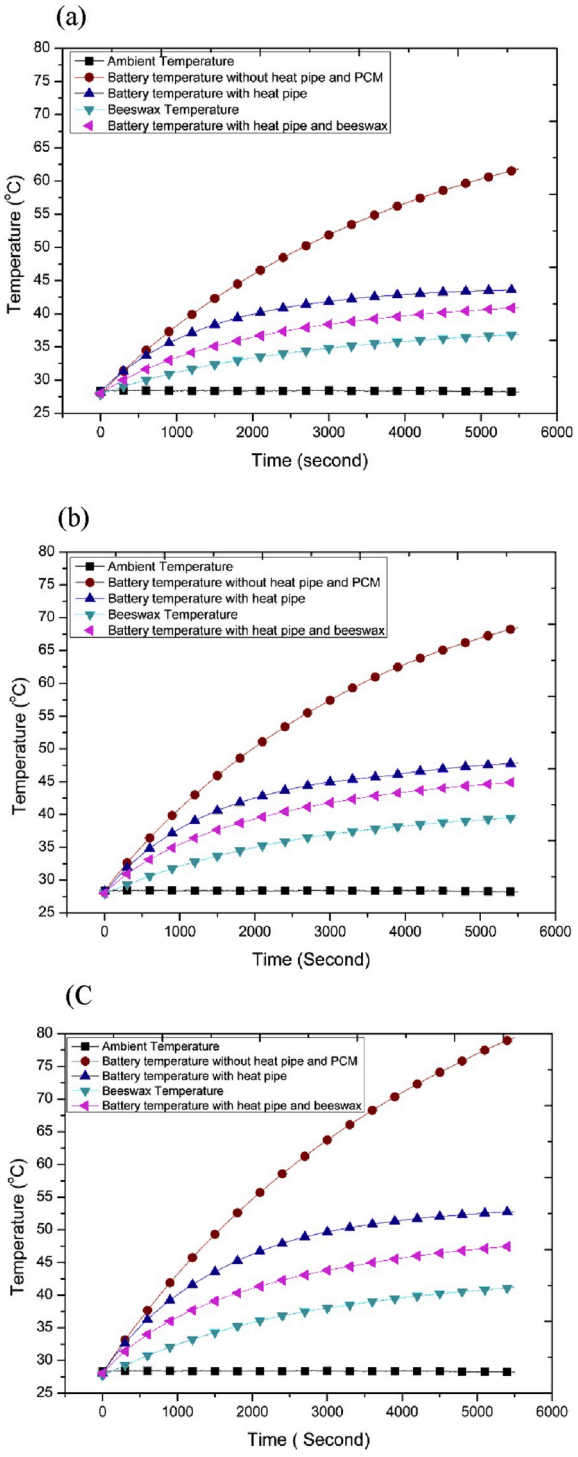

Fig. 3. Temperature distribution of battery surface with heat pipe and beeswax at different heat loads: a) 40 W, b) 50 W, and c) 60 W.

without heat pipes. Without heat pipes or PCM, the battery temperature needs a very long time to reach a steady-state condition. However, with heat pipe, the battery temperature reaches a steady-state condition at about 5500 s. Without heat pipe, the maximal battery surface temperatures at 40, 50, and 60 W were 60.9 °C, 67.1 °C, and 77.4 °C, respectively. The temperatures with heat pipe were 18.0 °C, 20.7 °C, and 26.6 °C lower, respectively. The presence of the heat pipes increased the heat transfer rate, thereby resulting in less internal energy of the battery simulator and a lower battery simulator temperature. Thus, the heat pipe effectively reduced the battery temperature.

Moreover, the higher the heating power, the lower was the temperature of the battery simulator. At higher temperatures, the heat pipes transferred more heat from the battery simulator to ambient air. However, the increase in heat transfer was smaller than the increase in heating power. The thermal resistance of the heat pipe decreased with increasing heat load: at 40, 50, and 60 W, the thermal resistances measured 0.108, 0.106, and 0.104 K/W, respectively. Putra et al. reported the same behavior for thermal resistance.

3.2. Heat pipe and beeswax PCM performance

In the next experiments, the heat pipe was covered with beeswax to further decrease the battery temperature. The melting temperature of beeswax is 62.2 °C, which exceeds the recommended temperature range of the battery. It will be more effective if the PCM has melting temperature point in the safe temperature range of battery. Although beeswax has a low thermal conductivity, it can store much thermal energy because it stores sensible and latent heat. Fig. 3 compares the battery temperatures obtained with a heat pipe and beeswax and those obtained with a heat pipe only.

The heat pipe and beeswax exhibited better performance than the heat pipe alone; the addition of beeswax to the battery simulators reduced the battery temperatures by 20.8 °C, 23.6 °C, and 31.9 °C, at heat loads of 40, 50, and 60 W, respectively. The beeswax enhanced the effect of the heat pipe by absorbing more heat from the battery. This phenomenon is attributed to the sensible heat of the beeswax rather than the latent heat because the working temperature of the battery was below the melting temperature of beeswax (Fig. 3). Furthermore, the beeswax temperature increased exponentially for 5500 s. Thus, the heat from the battery partially was absorbed by the beeswax.

The combination of the heat pipe and PCM exhibited better performance than the heat pipe alone. This is because during the heat exchange, the heat generated within the battery simulator was conducted through the PCM section and HP simultaneously. This heat was absorbed by the PCM and subsequently conducted through the conductor plate to the evaporator section and condenser section of the HP. The heat transfer and exchange process of this module is presented in Fig. 4. The three main steps are as follows: (1) The PCM absorbed and stored heat generated within the cells through sensible or latent heat storage during the phase change and transferred it to the assisted HP; (2) the assisted HP increased the heat absorption rate of the PCM; (3) the assisted HP dissipated heat from the battery simulator to the ambient air. Accordingly, to decrease the battery surface temperature, a PCM with relatively high thermal conductivity and an HP condenser section with a good heat exchange capacity are necessary to increase the thermal performance of the entire system.

Table 2 lists the total energy absorbed by the beeswax during the 5500 s. The recommended maximal working temperature of lithium-ion batteries is approximately 55 °C. The heat that can be absorbed by beeswax until the battery simulator temperature reaches 55 °C is 22.31 kJ. The battery simulator heat absorbed by the beeswax was 4.9% of the total heat generated by the heater. Therefore,

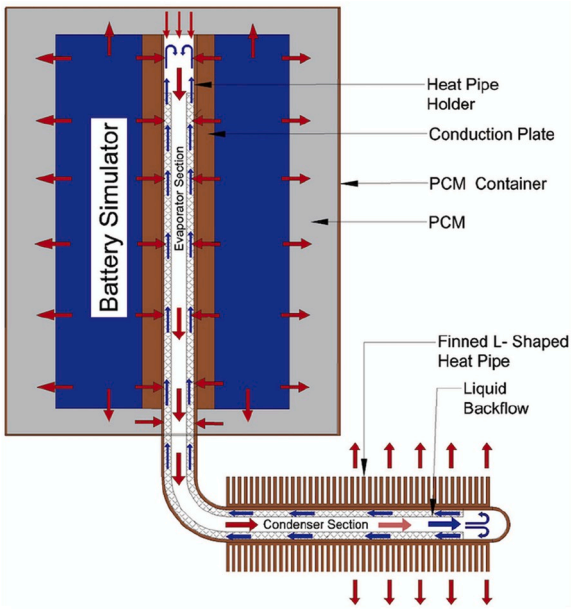

Fig. 4. Heat transfer and exchange process in heat pipe and PCM.

Table 2
Performance of beeswax as heat absorber.

No.	Heater power (W)	Beeswax temperature (°C)	*Q* Absorbed (kJ)
1	40	36.9	7.21
2	50	39.6	9.45
3	60	41.2	10.79

beeswax can be used in combination with heat pipes for passive battery cooling.

3.3. Heat pipe and RT 44 HC performance

The thermal properties of RT 44 HC differ from those of beeswax. The melting point of RT 44 HC is within the recommended battery temperature range. Fig. 5 shows the battery surface temperature when a heat pipe and RT 44 HC are used for passive cooling. The battery temperature obtained with heat pipe and RT 44 HC was lower than that with heat pipe and beeswax. Thus, the RT 44 HC absorbed more heat from the battery than the beeswax.

Moreover, the temperature reductions of the battery were 20.9 °C, 25.4 °C, and 33.2 °C for heat loads of 40, 50, and 60 W, respectively. At 40 W, the battery surface temperature was 39.5 °C. Thus, the RT 44 HC did not reach its melting point. As shown in Fig. 5(a), the temperature of RT 44 HC continued to increase during 5500 s. Thus, the heat was absorbed by sensible heat only. By contrast, when the heat load was 50 or 60 W [Fig. 5(b) and **(c)**], the temperature of RT 44 HC increased at the beginning and then remained constant at 38 °C. Thus, sensible and latent heats worked together to reduce the battery energy. Table 3 shows the heat absorbed by the RT 44 HC. It absorbed heat up to 18.7 kJ at low temperatures. Furthermore, the battery temperature could be maintained within the latent-heat temperature range of the RT 44 HC. The heat absorption did not cause its temperature to increase. Instead, the heat changed the phase of the RT 44 HC until it was completely melted.

3.4. Comparison of RT 44 HC and beeswax PCM performances

Battery cooling systems that combine heat pipes with beeswax or RT 44 HC can maintain the battery simulator temperature below 55 °C. In this study, the temperature of the RT 44 HC increased faster than that of beeswax in the sensible-heat region because the specific heat of RT 44 HC is lower than that of beeswax (specific heat of beeswax: 2081 kJ/kg.K; specific heat of RT 44 HC: 2,0 kJ/kg.K). In addition, the temperatures of beeswax and RT 44 HC exhibited different trends. As shown in Fig. 6, the temperature of beeswax increased until the process end, whereas the temperature of RT 44 HC remained constant at 38 °C. Furthermore, the RT 44 HC experienced a phase change at 38 °C. Thus, the temperature remained constant while the heat was absorbed from the battery simulator. Table 4 lists the properties of the RT 44 HC and beeswax performances. In order to compare to other researcher's results, Huang et al., showed that to reach the setting temperature, the heat pipe assisted PCM needs relatively longer working time than the present study. This is because of the difference in geometry, types of heat pipe and volume of PCM.

In this study, the RT 44 HC employed latent heat to absorb the battery heat. Compared with beeswax, the RT 44 HC absorbed more heat, which resulted in a greater battery temperature decrease. Thus, the combination of a PCM and heat pipe as a passive cooling system efficiently reduced the battery temperature and maintained it below 55 °C. The performance of the RT 44 HC was superior to that of beeswax because both sensible and latent heats were involved. According to Fig. 6, the combination of a heat pipe and RT 44 HC resulted in a battery simulator temperature that increased to 38 °C and remained constant afterward. The heat transfer below 38 °C was a sensible-heat transfer. Afterward, a latent-heat transfer occurred.

4. Conclusions

We investigated the effectiveness of combinations of heat pipes and PCMs as passive battery cooling systems with battery simulators. The results show that the heat pipes can reduce the battery temperature for different experimental heat energies with respect to a battery without a passive cooling system. The maximal reduction in the battery surface temperature was 26.6 °C for a heat load of 60 W. The use of heat pipes resulted in a quicker release of battery system heat to the ambient environment. Thus, the proper work temperature could be maintained, and the risk of overheating was lowered.

Adding a PCM to the heat pipe further enhanced the performance of the passive cooling system. Compared with the temperature without passive cooling, a combination of heat pipes with beeswax or RT 44 HC can reduce the battery simulator surface temperature by 31.9 °C or 33.2 °C, respectively. Thus, the PCMs effectively enhance the performance of the heat pipe as a passive battery cooling system by facilitating the heat absorption.

In addition, the RT 44 HC absorbed more heat from the battery simulator than the beeswax, thereby resulting in a greater reduction in the battery temperature. The superior performance of the RT 44 HC is attributed to its melting temperature, which is within the range of the battery working temperature. Thus, the RT 44 HC can use latent heat to store thermal energy. By contrast, beeswax can only use its sensible heat in the battery working temperature range.

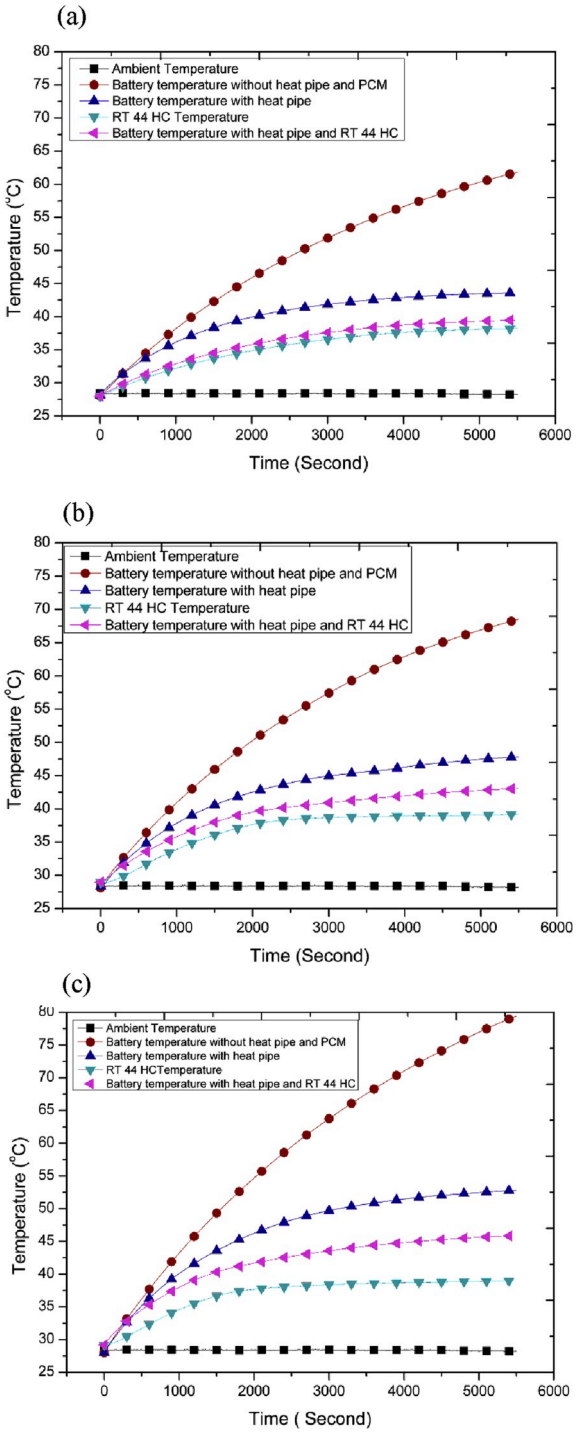

Fig. 5. Temperature distribution of Battery surface with heat pipe and RT 44 HC at different heat loads: a) 40 W, b) 50 W, and c) 60 W.

Declaration of competing interest

We have approved the manuscript and agree with submission to Applied Thermal Engineering. There are no conflicts of interest to declare. This manuscript has not been published elsewhere and is not under consideration by another journal.

Table 3
Performance of heat pipe with RT 44 HC

No.	Heater power (W)	RT 44 HC temperature (°C)	Q Absorbed (kJ)
1	40	38.2	8.0
2	50	38.7	14.3
3	60	39.2	18.6

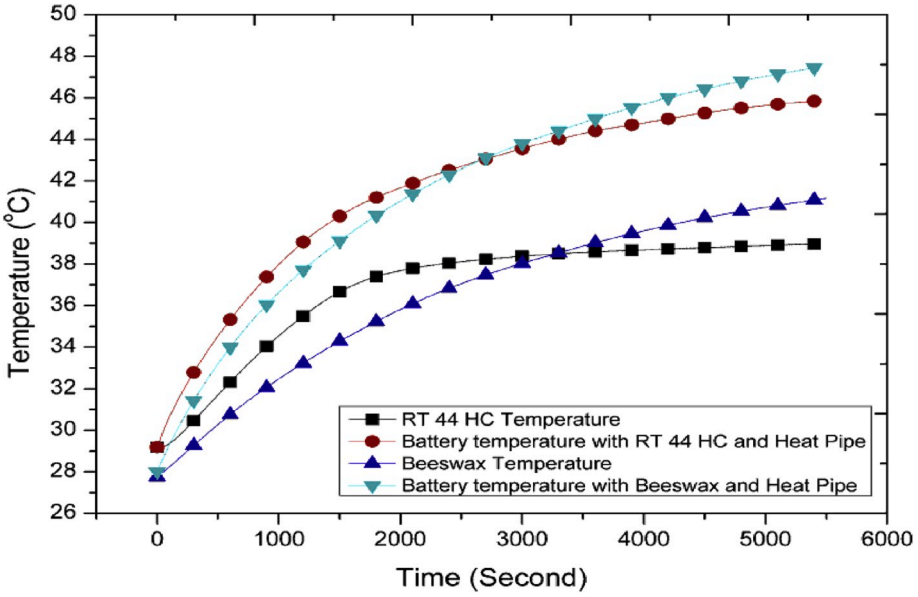

Fig. 6. Comparison of battery surface temperatures for heat load of 60 W.

Table 4
Comparison of RT 44 HC and beeswax performances.

Cooling system	Battery temperature (°C)	Battery temperature drop (°C)	Absorbed energy (kJ)
RT 44 HC + heat pipe	39.5	20.89	8.025
	43.08	25.42	14.261
	45.85	33.19	18.55
Beeswax + heat pipe	40.81	20.75	7.208
	44.9	23.57	9.447
	47.45	31.93	10.787

CRediT authorship contribution statement

Nandy Putra: Conceptualization, Methodology, Supervision. **Adjie Fahrizal Sandi:** Investigation, Visualization. **Bambang Ariantara:** Writing - original draft, Visualization. **Nasruddin Abdullah:** Data curation, Validation. **Teuku Meurah Indra Mahlia:** Writing - review & editing.

Acknowledgments

The authors thank the Directorate of Research and Community Service, Universitas Indonesia, for funding this research project under the Q1Q2 Program 2019, no. NKB-0315/UN2.R3.1/HKP05.00/2019.

References

[1] R.S. Norhasyima, T.M.I. Mahlia, Advances in CO2 utilization technology: a patent landscape review, Journal of Co2 Utilization 26 (2018) 323–335.
[2] M.S. Ismail, M. Moghavvemi, T.M.I. Mahlia, Techno-economic analysis of an optimized photovoltaic and diesel generator hybrid power system for remote houses in a tropical climate, Energy Convers. Manag. 69 (2013) 163–173.
[3] M.S. Ismail, M. Moghavvemi, T.M.I. Mahlia, Genetic algorithm based optimization on modeling and design of hybrid renewable energy systems, Energy Convers. Manag. 85 (2014) 120–130.

[4] A.S. Silitonga, T.M.I. Mahlia, F. Kusumo, S. Dharma, A.H. Sebayang, R.W. Sembiring, et al., Intensification of Reutealis trisperma biodiesel production using infrared radiation: simulation, optimisation and validation, Renew. Energy 133 (2019) 520–527.
[5] P. Barla, S. Proost, Energy efficiency policy in a non-cooperative world, Energy Econ. 34 (2012) 2209–2215.
[6] C. Strickland, R. Sturm, Energy efficiency in World Bank power sector policy and lending New opportunities, Energy Pol. 26 (1998) 873–883.
[7] M. Uddin, K. Techato, J. Taweekun, M. Rahman, M. Rasul, T. Mahlia, et al., An overview of recent developments in biomass pyrolysis technologies, Energies 11 (2018) 3115.
[8] S.T. Latibari, M. Mehrali, M. Mehrali, T.M.I. Mahlia, H.S.C. Metselaar, Synthesis, characterization and thermal properties of nanoencapsulated phase change materials via sol-gel method, Energy 61 (2013) 664–672.
[9] M. Mehrali, S.T. Latibari, M. Mehrali, T.M.I. Mahlia, H.S.C. Metselaar, M.S. Naghavi, et al., Preparation and characterization of palmitic acid/graphene nanoplatelets composite with remarkable thermal conductivity as a novel shape-stabilized phase change material, Appl. Therm. Eng. 61 (2013) 633–640.
[10] M. Amin, N. Putra, E.A. Kosasih, E. Prawiro, R.A. Luanto, T.M.I. Mahlia, Thermal properties of beeswax/graphene phase change material as energy storage for building applications, Appl. Therm. Eng. 112 (2017) 273–280.
[11] N. Putra, Hakim II, F.P. Erwin, N.A. Abdullah, B. Ariantara, M. Amin, et al., Development of a novel thermoelectric module based device for thermal stability measurement of phase change materials, Journal of Energy Storage 22 (2019) 331–335.
[12] N. Putra, S. Rawi, M. Amin, E. Kusrini, E.A. Kosasih, T.M.I. Mahlia, Preparation of beeswax/multi-walled carbon nanotubes as novel shape-stable nanocomposite phase-change material for thermal energy storage, Journal of Energy Storage 21 (2019) 32–39.
[13] J.D. Malaczynski, T.P. Duane, Reducing greenhouse gas emissions from vehicle miles traveled: integrating the California environmental quality act with the California global warming solutions act, Ecol. Law Q. 36 (2009) 71–135.
[14] M. Mahdavi, S. Tiari, S. De Schampheleire, S. Qiu, Experimental study of the thermal characteristics of a heat pipe, Exp. Therm. Fluid Sci. 93 (2018) 292–304.
[15] T.-H. Tran, S. Harmand, B. Desmet, S. Filangi, Experimental investigation on the feasibility of heat pipe cooling for HEV/EV lithium-ion battery, Appl. Therm. Eng. 63 (2014) 551–558.
[16] H. Akeiber, P. Nejat, M.Z.A. Majid, M.A. Wahid, F. Jomehzadeh, I.Z. Famileh, et al., A review on phase change material (PCM) for sustainable passive cooling in building envelopes, Renew. Sustain. Energy Rev. 60 (2016) 1470–1497.
[17] F.F. Bai, M.B. Chen, W.J. Song, Z.P. Feng, Y.L. Li, Y.L. Ding, Thermal management performances of PCM/water cooling-plate using for lithium-ion battery module based on non-uniform internal heat source, Appl. Therm. Eng. 126 (2017) 17–27.
[18] Chen HB, Cao HZ, Li HX, Zhao XW, Liu XF. Experimental study on coupled cooling system of PCM-heat pipe for vehicle power battery pack. In: Chan K, Yeh J, editors. Proceedings of the 2015 International Conference on Electrical, Automation and Mechanical Engineering 2015. p. 454-457.
[19] L.W. Fan, J.M. Khodadadi, A.A. Pesaran, A parametric study on thermal management of an air-cooled lithium-ion battery module for plug-in hybrid electric vehicles, J. Power Sources 238 (2013) 301–312.
[20] S.K. Mohammadian, Y.W. Zhang, Thermal management optimization of an air-cooled Li-ion battery module using pin-fin heat sinks for hybrid electric vehicles, J. Power Sources 273 (2015) 431–439.
[21] Z. Rao, Z. Qian, Y. Kuang, Y. Li, Thermal performance of liquid cooling based thermal management system for cylindrical lithium-ion battery module with variable contact surface, Appl. Therm. Eng. 123 (2017) 1514–1522.
[22] K. Li, J. Yan, H. Chen, Q. Wang, Water cooling based strategy for lithium ion battery pack dynamic cycling for thermal management system, Appl. Therm. Eng. 132 (2018) 575–585.
[23] X.M. Xu, J.Q. Fu, R.J. Ding, H.F. Jin, Y. Xiao, Heat dissipation performance of electric vehicle battery liquid cooling system with double-inlet and double-outlet channels, J. Renew. Sustain. Energy 10 (2018).
[24] N. Putra, B. Ariantara, R.A. Pamungkas, Experimental investigation on performance of lithium-ion battery thermal management system using flat plate loop heat pipe for electric vehicle application, Appl. Therm. Eng. 99 (2016) 784–789.
[25] R. McGlen, P. Kew, D. Reay, Heat Pipes: Theory, Design and Applications, Elsevier, 2006.
[26] Z. Rao, Q. Wang, C. Huang, Investigation of the thermal performance of phase change material/mini-channel coupled battery thermal management system, Appl. Energy 164 (2016) 659–669.
[27] Z. Wang, H. Zhang, X. Xia, Experimental investigation on the thermal behavior of cylindrical battery with composite paraffin and fin structure, Int. J. Heat Mass Tran. 109 (2017) 958–970.
[28] W. Wu, X. Yang, G. Zhang, X. Ke, Z. Wang, W. Situ, et al., An experimental study of thermal management system using copper mesh-enhanced composite phase change materials for power battery pack, Energy 113 (2016) 909–916.
[29] Q.Q. Huang, X.X. Li, G.Q. Zhang, J.Y. Zhang, F.Q. He, Y. Li, Experimental investigation of the thermal performance of heat pipe assisted phase change material for battery thermal management system, Appl. Therm. Eng. 141 (2018) 1092–1100.
[30] W. Wu, X. Yang, G. Zhang, K. Chen, S. Wang, Experimental investigation on the thermal performance of heat pipe-assisted phase change material based battery thermal management system, Energy Convers. Manag. 138 (2017) 486–492.
[31] W. Zhang, J. Qiu, X. Yin, D. Wang, A novel heat pipe assisted separation type battery thermal management system based on phase change material, Appl. Therm. Eng. 165 (2020) 114571.
[32] D. Peckner, I.M. Bernstein, McGraw-Hill Book Company, New York, 1977.
[33] M.H. Kusuma, N. Putra, A.R. Antariksawan, Susyadi, F.A. Imawan, Investigation of the thermal performance of a vertical two-phase closed thermosyphon as a passive cooling system for a nuclear reactor spent fuel storage pool, Nuclear Engineering and Technology 49 (2017) 476–483.
[34] S. Motahar, R. Khodabandeh, Experimental study on the melting and solidification of a phase change material enhanced by heat pipe, Int. Commun. Heat Mass Tran. 73 (2016) 1–6.